J|A|C|S
ARTICLES

Published on Web 10/29/2008

SERS-Melting: A New Method for Discriminating Mutations in DNA Sequences

Sumeet Mahajan, James Richardson, Tom Brown, and Philip N. Bartlett*

School of Chemistry, University of Southampton, Southampton SO17 1BJ, United Kingdom

Received July 16, 2008; E-mail: pnb@soton.ac.uk

Abstract: The reliable discrimination of mutations, single nucleotide polymorphisms (SNPs), and other differences in genomic sequence is an essential part of DNA diagnostics and forensics. It is commonly achieved using fluorescently labeled DNA probes and thermal gradients to distinguish between the matched and mismatched DNA. Here, we describe a novel method that uses surface enhanced (resonance) Raman spectroscopy (SER(R)S) to follow denaturation of dsDNA attached to a structured gold surface. This denaturation is driven either electrochemically or thermally on SERS active sphere segment void (SSV) gold substrates. Using this method, we can distinguish between wild type, a single point mutation (1653C/T), and a triple deletion (ΔF 508) in the CFTR gene at the 0.02 attomole level, and the method can be used to differentiate the unpurified PCR products of the wild type and ΔF 508 mutation. Our method has the potential to provide small, rapid, sensitive, reproducible platforms for detecting genetic variations and sequencing genes.

Introduction

The development of simple, reliable, high-throughput methods to detect genetic variations in DNA is crucial for the development of DNA-based diagnostics and forensics. A variety of methods for identifying mutations[1] have been described in the literature using either solution-based or surface methods. Solution-based methods include the identification of single-strand conformational polymorphism,[2,3] use of denaturing gradient gel electrophoresis,[2,4] or quantitative polymerase chain reaction-based approaches. The latter have the advantages that they do not require a chromatographic separation step and that they can be used to detect several sequences simultaneously. The most widely used methods are based on fluorescent detection schemes such as those used in Molecular Beacons,[5] Taqman,[6] Scorpions,[7] or Hybridization Probes.[8]

The use of surface-based approaches offers the attraction of an array approach to the detection of mutations, the opportunity to control the conditions locally at the surface, and the ability to produce simple, portable biosensor devices. A variety of sensing approaches have been investigated including the measurement of mass changes using a quartz crystal microbalance,[9,10] nanomechanical detection using microcantilevers,[11] local refractive index changes using surface plasmon resonance,[12,13] electrochemical changes[14−16] using either impedance measurements[17−20] or redox labels,[21−26] and fluorescence;[27−29] of these, only a few utilize differential denaturation (melting analysis) on solid substrates.[13]

In a typical solid-phase analytical system relying on differential denaturation analysis, a single-strand DNA (ssDNA)

(1) Nollau, P.; Wagener, C. *Clin. Chem.* **1997**, *43*, 1114.
(2) Bernat, M.; Titos, E.; Clària, J. *Genet. Mol. Res.* **2002**, *1*, 72.
(3) Orita, M.; Iwahana, H.; Kanazawa, H.; Hayashi, K.; Sekiya, T. *Proc. Natl. Acad. Sci. U.S.A.* **1989**, *86*, 2766.
(4) Myers, R.; Fischer, S.; Lerman, L.; Maniatis, T. *Nucleic Acids Res.* **1985**, *13*, 3131.
(5) Tyagi, S.; Kramer, F. R. *Nat. Biotechnol.* **1996**, *14*, 303.
(6) Holland, P. M.; Abramson, R. D.; Watson, R.; Gelfand, D. H. *Proc. Natl. Acad. Sci. U.S.A.* **1991**, *88*, 7276.
(7) Whitcombe, D.; Theaker, J.; Guy, S. P.; Brown, T.; Little, S. *Nat. Biotechnol.* **1999**, *17*, 804.
(8) Wittwer, C. T.; Herrmann, M. G.; Moss, A. A.; Rasmussen, R. P. *BioTechniques* **1997**, *22*, 130.
(9) Caruso, F.; Rodda, E.; Furlong, D. N.; Niikura, K.; Okahata, Y. *Anal. Chem.* **1997**, *69*, 2043.
(10) Okahata, Y.; Kawase, M.; Niikura, K.; Ohtake, F.; Furusawa, H.; Ebara, Y. *Anal. Chem.* **1998**, *70*, 1288.
(11) McKendry, R.; Zhang, J. Y.; Arntz, Y.; Strung, T.; Hegner, M.; Lang, H. P.; Baller, M. K.; Certa, U.; Meyer, E.; Guntherodt, H. J.; Gerber, C. *Proc. Natl. Acad. Sci. U.S.A.* **2002**, *99*, 9783.
(12) Nakatani, K.; Sando, S.; Saito, I. *Nat. Biotechnol.* **2001**, *19*, 51.
(13) Thiel, A. J.; Frutos, A. G.; Jordan, C. E.; Corn, R. M.; Smith, L. M. *Anal. Chem.* **1997**, *69*, 4948.
(14) Gooding, J. J. *Electroanalysis* **2002**, *14*, 1149.
(15) Kerman, K.; Kobayashi, M.; Tamiya, E. *Meas. Sci. Technol.* **2004**, *15*, R1.
(16) Drummond, T. G.; Hill, M. G.; Barton, J. K. *Nat. Biotechnol.* **2003**, *21*, 1192.
(17) Li, X.; Lee, J. S.; Kraatz, H.-B. *Anal. Chem.* **2006**, *78*, 6096.
(18) Lee, T.; Shim, Y. *Anal. Chem.* **2001**, *73*, 5629.
(19) Li, C. Z.; Long, Y. T.; Lee, J. S.; Kraatz, H. B. *Chem. Commun.* **2004**, 574.
(20) Long, Y.-T.; Li, C.-Z.; Sutherland, T. C.; Kraatz, H.-B.; Lee, J. S. *Anal. Chem.* **2004**, *76*, 4059.
(21) Hashimoto, K.; Ito, K.; Ishlmori, Y. *Anal. Chem.* **1994**, *66*, 3830.
(22) Ihara, T.; Nakayama, M.; Murata, M.; Nakano, K.; Maeda, M. *Chem. Commun.* **1997**, 1609.
(23) Millan, K. M.; Mikkelsen, S. R. *Anal. Chem.* **1993**, *65*, 2317.
(24) Paleček, E.; Masařı´k, M.; Kizek, R.; Kuhlmeier, D.; Hassmann, J.; Schülein, J. *Anal. Chem.* **2004**, *76*, 5930.
(25) Wang, J.; Xu, D.; Kawde, A.; Polsky, R. *Anal. Chem.* **2001**, *73*, 5576.
(26) Yu, C. J.; Wan, Y.; Yowanto, H.; Li, J.; Tao, C.; James, M. D.; Tan, C. L.; Blackburn, G. F.; Meade, T. J. *J. Am. Chem. Soc.* **2001**, *123*, 11155.
(27) Ramachandran, A.; Flinchbauch, J.; Ayoubi, P.; Olah, G. A.; Malayer, J. R. *Biosens. Bioelectron.* **2003**, *19*, 727.
(28) Du, H.; Strohsahl, C. M.; Camera, J.; Miller, B. L.; Krauss, T. D. *J. Am. Chem. Soc.* **2005**, *127*, 7932.
(29) Wang, H.; Li, J.; Liu, H.; Liu, Q.; Mei, Q.; Wang, Y.; Zhu, J.; He, N.; Lu, Z. *Nucleic Acids Res.* **2002**, *30*, e61.

probe is immobilized on the substrate and then hydridized to "target" sequences from solution. The resulting DNA duplexes are then denatured, typically either by ramping the temperature or by washing with solutions of decreasing ionic strength (stringency washing). Mutations are detected by monitoring the denaturation process; the mutations possess base pair mismatches, which destabilize the duplex relative to the perfectly complementary target, and therefore these duplexes denature more readily.

Although optical wave guides,[30] optical scan arrays,[31] and temperature gradient assay platforms[32] have been employed, fluorescence is currently the preferred technique for detecting mutations using this hybridization/denaturation strategy.[33] However, surface-enhanced Raman or resonant Raman scattering (SER(R)S) has been shown to possess significant advantages as compared to fluorescence;[34−36] these include the ability to multiplex because of the narrow line width (∼10 nm) and molecular specificity of SER(R) spectra,[35,37] flexibility in the choice of labels,[38−40] insensitivity to quenching by oxygen or other species,[34] and excellent sensitivity.[38] In addition, SER(R)S has the benefit of using a single excitation wavelength without imposing any inflexibility on the choice of donor, which is the case in FRET (Forster or fluorescence resonance energy transfer). When compared to surface-plasmon resonance (SPR)[13] or electrochemical detection methods,[16] SER(R)S is molecule-specific and much more sensitive. Finally, SER(R)S is a highly surface-sensitive technique so that there is no significant interference from species that are not at or close to (typically <100 nm) the surface.

The application of SERS to analysis of DNA was pioneered by Vo-Dinh and colleagues[41] using rough silver surfaces formed by thermal evaporation of thin silver films onto 100 nm alumina particles dropped coated on glass. In these original experiments, DNA was hybridized on nitrocellulose membranes, and then the labeled double-stranded DNA was spotted onto the SERS substrate for analysis. In subsequent studies, they showed that SERS detection could be used on DNA arrays with multispectral imaging[42] and when the DNA probes were attached to the SERS active rough silver surface.[36,43,44] Flocculated silver colloids have also been used very successfully by Graham, Smith, and their colleagues for SER(R)S detection of DNA, including the use of different labels for multiplex geneotyping,[45] quantitative SERRS using two wavelengths and different dyes,[46,47] and the development of SERRS beacons.[48] In their recent work, they have shown that the same methods can be used on a commercially available structured gold surface.[49]

In our laboratory, we have been developing the fabrication of ordered sphere segment void (SSV) substrates by electrodeposition around templates made from close packed monolayers of uniform submicrometer diameter polystyrene spheres.[50] Removal of the polystyrene template by dissolution in a suitable solvent leaves a smooth sculpted metal surface with low surface roughness. We have studied the reflection spectra of these structures in detail[51−55] and shown that these metamaterials generate intense local electric fields under illumination and that, as a result, they are excellent substrates for SERS.[52,56] The optical properties of these substrates can be tuned[57,58] through the choice of sphere diameter and film thickness so that typical surface enhancements of the order of 10^6 have been demonstrated for structured gold substrates.[59] The sensitivity of detection can be further increased by selecting molecules that have an electronic transition in resonance with the laser excitation so that the surface enhancement is accompanied by a further resonant enhancement of $\sim 10^3$ to give surface-enhanced resonance Raman scattering (SERRS).[60] These SSV surfaces show excellent stability in solution and can be used as electrodes and still give stable repeatable SER(R)S.[61] The SSV surfaces differ in their structure from both the nanotriangle surfaces[62] and the metal film on nanosphere (MFON) surfaces[63] produced by Van Duyne and co-workers using similar colloidal particle templates. In the case of the SSV surfaces, both the sphere diameter and the film thickness can be varied independently to control the optical properties.

(30) Stimpson, D. I.; Hoijer, J. V.; Hsieh, W. T.; Jou, C.; Gordon, J.; Theriault, T.; Gamble, R.; Baldeschwieler, J. D. *Proc. Natl. Acad. Sci. U.S.A.* **1995**, *92*, 6379.
(31) Khomyakova, E. B.; Dreval, E. V.; Tran-Dang, M.; Potier, M. C.; Soussaline, F. P. *Cell. Mol. Biol.* **2004**, *50*, 217.
(32) Mao, H.; Holden, M. A.; You, M.; Cremer, P. S. *Anal. Chem.* **2002**, *74*, 5071.
(33) Ranasinghe, R. T.; Brown, T. *Chem. Commun.* **2005**, 5487.
(34) Braun, G.; Lee, S. J.; Dante, M.; Nguyen, T. Q.; Moskovits, M.; Reich, N. *J. Am. Chem. Soc.* **2007**, *129*, 6378.
(35) Cao, Y. C.; Jin, R.; Mirkin, C. A. *Science* **2002**, 1536.
(36) Culha, M.; Stokes, D.; Allain, L. R.; Vo-Dinh, T. *Anal. Chem.* **2003**, *75*, 6196.
(37) Stokes, R. J.; Macaskill, A.; Lundahl, P. J.; Smith, W. E.; Faulds, K.; Graham, D. *Small* **2007**, *3*, 1593.
(38) Faulds, K.; Barbagallo, R. P.; Keer, J. T.; Smith, W. E.; Graham, D. *Analyst* **2004**, *129*, 567.
(39) Faulds, K.; Smith, W. E.; Graham, D. *Anal. Chem.* **2004**, *76*, 412.
(40) Graham, D.; Smith, W. E.; Linacre, A. M. T.; Munro, C. H.; Watson, N. D.; White, P. C. *Anal. Chem.* **1997**, *69*, 4703.
(41) Vo-Dinh, T.; Houck, K.; Stokes, D. L. *Anal. Chem.* **1994**, *66*, 3379.
(42) Vo-Dinh, T.; Stokes, D. L.; Griffin, G. D.; Volkan, M.; Kim, U. J.; Simon, M. I. *J. Raman Spectrosc.* **1999**, *30*, 785.
(43) Isola, N. R.; Stokes, D. L.; Vo-Dinh, T. *Anal. Chem.* **1998**, *70*, 1352.
(44) Vo-Dinh, T.; Allain, L. R.; Stokes, D. L. *J. Raman Spectrosc.* **2002**, *33*, 511.
(45) Graham, D.; Mallinder, B. J.; Whitcombe, D.; Watson, N. D.; Smith, W. E. *Anal. Chem.* **2002**, *74*, 1069.
(46) Faulds, K.; Stewart, L.; Smith, W. E.; Graham, D. *Talanta* **2005**, *67*, 667.
(47) Faulds, K.; McKenzie, F.; Smith, W. E.; Graham, D. *Angew. Chem., Int. Ed.* **2007**, *46*, 1829.
(48) Faulds, K.; Fruk, L.; Robson, D. C.; Thompson, D. G.; Enright, A.; Smith, W. E.; Graham, D. *Faraday Discuss.* **2006**, *132*, 261.
(49) Stokes, R. J.; Macaskill, A.; Dougan, J. A.; Hargreaves, P. G.; Stanford, H. M.; Smith, W. E.; Faulds, K.; Graham, D. *Chem. Commun.* **2007**, 2811.
(50) Bartlett, P. N.; Baumberg, J. J.; Birkin, P. R.; Ghanem, M. A.; Netti, M. C. *Chem. Mater.* **2002**, *14*, 2199.
(51) Netti, M. C.; Coyle, S.; Baumberg, J. J.; Ghanem, M. A.; Birkin, P. R.; Bartlett, P. N.; Whitaker, D. M. *Adv. Mater.* **2001**, *13*, 1368.
(52) Kelf, T. A.; Sugawara, Y.; Baumberg, J. J.; Abdelsalam, M.; Bartlett, P. N. *Phys. Rev. Lett.* **2005**, *95*, 116802.
(53) Kelf, T. A.; Sugawara, Y.; Cole, R. M.; Baumberg, J. J.; Abdelsalam, M. E.; Cintra, S.; Mahajan, S.; Russell, A. E.; Bartlett, P. N. *Phys. Rev. B* **2006**, *74*, 245415.
(54) Bartlett, P. N.; Baumberg, J. J.; Coyle, S.; Abdelsalem, M. *Faraday Discuss.* **2004**, *125*, 117.
(55) Cole, R. M.; Baumberg, J. J.; Abajo, F. J. G. d.; Mahajan, S.; Abdelsalam, M.; Bartlett, P. N. *Nano Lett.* **2007**, *7*, 2094.
(56) Abdelsalam, M. E.; Bartlett, P. N.; Baumberg, J. J.; Cintra, S.; Kelf, T.; Russell, A. E. *Electrochem. Commun.* **2005**, *7*, 740.
(57) Baumberg, J. J.; Kelf, T.; Sugawara, Y.; Cintra, S.; Abdelsalam, M.; Bartlett, P. N.; Russell, A. E. *Nano Lett.* **2005**, 2262.
(58) Mahajan, S.; Abdelsalam, M.; Suguwara, Y.; Cintra, S.; Russell, A.; Baumberg, J.; Bartlett, P. *Phys. Chem. Chem. Phys.* **2007**, *9*, 104.
(59) Cintra, S.; Abdelsalem, M.; Bartlett, P. N.; Baumberg, J. J.; Kelf, T.; Sugawara, Y.; Russell, A. E. *Faraday Discuss.* **2005**, *132*, 191.
(60) Mahajan, S.; Baumberg, J.; Russell, A.; Bartlett, P. *Phys. Chem. Chem. Phys.* **2007**, *9*, 6016.
(61) Abdelsalam, M.; Bartlett, P. N.; Russell, A. E.; Baumberg, J. J.; Calvo, E. J.; Tognalli, N. G.; Fainstein, A. *Langmuir* **2008**, *24*, 7018.
(62) Haynes, C. L.; Van Duyne, R. P. *J. Phys. Chem. B* **2001**, *105*, 5599.
(63) Dick, L. A.; McFarland, A. D.; Haynes, C. L.; Van Duyne, R. P. *J. Phys. Chem. B* **2002**, *106*, 853.

Although advances have been made in the application of SERS for DNA diagnostics by hybridization to surface bound probes,[36,43−45] including techniques that avoid direct labeling of the target sequences by using molecular beacons[48] or silver nanoparticles,[34] none of these methods have been used in dsDNA melting studies to discriminate between mutations. In this Article, we describe the use of SERS combined with either thermal or electrochemical cycling to discriminate mutations. Although there are a few reports of mutation detection by monitoring temperature- or potential-induced denaturation using SPR,[64,65] to date fluorescence monitoring remains the dominant technique with several systems commercially available.[66,67] The use of an applied electric field to affect hybridization and to determine mutations by the application of a constant potential (−300 mV) followed by measuring the change in fluorescence with time has been described by Sosnowski et al.[68] In their work, the probes were immobilized in a 1 μm thick gel-permeation layer coating the electrode, and denaturation was brought about by a complex mechanism involving a mixture of effects rather than as the result of simple electrostatic repulsion at the metal surface.[69,70] The use of electrochemical scanning dehybridization using fluorescence monitoring for SNP recognition has been recently demonstrated on silicon substrates with surface-bound hairpin (molecular beacons) probes.[71,72] However, in these experiments, the authors were unable to generate sufficient difference to distinguish SNP targets from the perfect match when using linear DNA probes. There are also a few reports on monitoring electrochemical denaturation with other techniques such as SPR[64] and chemiluminescence[73] in which a constant potential was applied[68] and denaturation was monitored with time.

In this work, we show that the SSV substrates can be used to obtain stable reproducible SERS signals for labeled ssDNA during hybridization onto surface attached DNA probe sequences. We show that these target sequences can be melted from the surface and rehybridized and that the method is highly sensitive with detection at sub attomole levels. Further, sequences in the gene responsible for coding the Cystic Fibrosis Transmembrane Regulator (CFTR) protein were used as a model system to demonstrate the discrimination of different mutations. Mutations in this gene cause cystic fibrosis, which is one of the most common inherited genetic life-shortening diseases, reducing the life expectancy to 37.5 years, across different populations.[74] Two particular mutations, ΔF 508 the most common CFTR mutation (70% and 90% of cystic fibrosis cases in U.K. and U.S., respectively) and 1653C/T a relatively rare single point mutation occurring in the same gene fragment, were targeted. We show that we can distinguish between the wild type, the single nucleotide mutation, and the most common triplet deletion in the human CFTR gene by employing SER(R)S to follow melting of the dsDNA from the SSV surface as either the temperature or the applied potential is scanned. Finally, we demonstrate the applicability of this approach in real systems by discriminating between the unpurified amplicons of the wild type and triplet deletion in the human CFTR gene following asymmetric PCR of a DNA sample.

Experimental Section

Fabrication of Substrates. For a typical fabrication procedure, glass microscope slides were coated with a 10 nm chromium adhesion layer followed by 200 nm of gold using standard thermal evaporation. 2 cm × 1.5 cm pieces were cut from the gold-coated slide, cleaned by sonicating in isopropanol for 90 min, washed, and dipped in 10 mM cysteamine in ethanol for at least 48 h. Subsequently, these treated surfaces are washed with water and assembly of polystyrene spheres (obtained as 1% solutions from Duke Scientific) was carried out. This served as the template for the formation of sphere segment voids. Electrodeposition was carried out using a commercial gold electroplating bath (ECF 60, Technic Inc.) to which an additive (Brightener E3, Technic Inc.) was added for a bright and smooth finish. A fixed area was masked, and the charge required for a particular height was calculated. Electrodeposition was carried under potentiostatic control at −0.73 V versus a homemade saturated calomel electrode (SCE) with a platinum counter electrode. The deposition was terminated when the requisite amount of charge had been passed. The polystyrene spheres were then removed by dissolution in DMF to obtain ordered sphere segment void substrates. In the present work, 600 nm diameter spheres were employed, and the gold film was electrodeposited to 480 nm.

Oligonucleotide Synthesis. Standard DNA phosphoramidites, solid supports, and additional reagents were purchased from Link Technologies Ltd., Sigma, and Applied Biosystems Ltd. For 3′-labeling, C7-aminoalkyl and C7-fluorescein (FAM) synthesis columns were obtained from Link Technologies Ltd., and Cy3, Cy5, and dithiol phosphoramidites were purchased from Glen Research Inc. All oligonucleotides were synthesized on an Applied Biosystems 394 automated DNA/RNA synthesizer using standard 0.2 or 1.0 μmol phosphoramidite cycles of acid-catalyzed detritylation, coupling, capping, and iodine oxidation. Stepwise coupling efficiencies and overall yields were determined by the automated trityl cation conductivity monitoring facility and in all cases were >98.0%. All β-cyanoethyl phosphoramidite monomers were dissolved in anhydrous acetonitrile to a concentration of 0.1 M immediately prior to use. The coupling time for normal (A, G, C, T) monomers was 25 s, and the coupling time for the Cy3, Cy5, and dithiol monomers was extended to 360 s. Cleavage of oligonucleotides from the solid support and deprotection was achieved by exposure to concentrated aqueous ammonia for 60 min at room temperature followed by heating in a sealed tube for 5 h at 55 °C. Oligonucleotides labeled with 5′-Cy3 and 5′-Cy5 were prepared by adding the appropriate Cy phosphoramidite monomer at the final addition in solid-phase synthesis. The Cy3 and Cy5 chromophores are unstable to prolonged exposure to ammonia, so 5′-Cy oligonucleotides were synthesized using fast deprotecting dmf-G and Ac-dC phosphoramidite monomers, cleaved from the resin by treatment with concentrated aqueous ammonia for 60 min

(64) Heaton, R. J.; Peterson, A. W.; Georgiadis, R. M. *Proc. Natl. Acad. Sci. U.S.A.* **2001**, *98*, 3701.
(65) Peterlinz, K. A.; Georgiadis, R. M.; Herne, T. M.; Tarlov, M. J. *J. Am. Chem. Soc.* **1997**, *119*, 3401.
(66) Herrmann, M. G.; Durtschi, J. D.; Wittwer, C. T.; Voelkerding, K. V. *Clin. Chem.* **2007**, *53*, 1544.
(67) Meuzelaar, L. S.; Hopkins, K.; Liebana, E.; Brookes, A. J. *J. Mol. Diagn.* **2007**, *9*, 30.
(68) Sosnowski, R. G.; Tu, E.; Butler, W. F.; O'Connell, J. P.; Heller, M. J. *Proc. Natl. Acad. Sci. U.S.A.* **1997**, *94*, 1119.
(69) Kassegne, S. K.; Reese, H.; Hodko, D.; Yang, J. M.; Sarkar, K.; Smolko, D.; Swanson, P.; Raymond, D. E.; Heller, M. J.; Madou, M. J. *Sens. Actuators, B* **2003**, *94*, 81.
(70) Edman, C. F.; Raymond, D. E.; Wu, D. J.; Tu, E.; Sosnowski, R. G.; Butler, W. F.; Nerenberg, M.; Heller, M. J. *Nucleic Acids Res.* **1997**, *25*, 4907.
(71) Wei, F.; Chen, C. L.; Zhai, L.; Zhang, N.; Zhao, X. S. *J. Am. Chem. Soc.* **2005**, *127*, 5306.
(72) Wei, F.; Qu, P.; Zhai, L.; Chen, C. L.; Wang, H. F.; Zhao, X. S. *Langmuir* **2006**, *22*, 6280.
(73) Spehar-Deleze, A. M.; Schmidt, L.; Neier, R.; Kulmala, S.; de Rooij, N.; Koudelka-Hep, M. *Biosens. Bioelectron.* **2006**, *22*, 722.
(74) Kerem, B.-S.; Rommens, J. M.; Buchanan, J. A.; Markiewicz, D.; Cox, T. K.; Chakravarti, A.; Buchwald, M.; Tsui, L.-C. *Science* **1989**, *245*, 1073.

Scheme 1. Structures of (a) Cy3, (b) Cy5, and (c) Texas Red Labels Coupled to the 3′ End of the Oligonucleotide

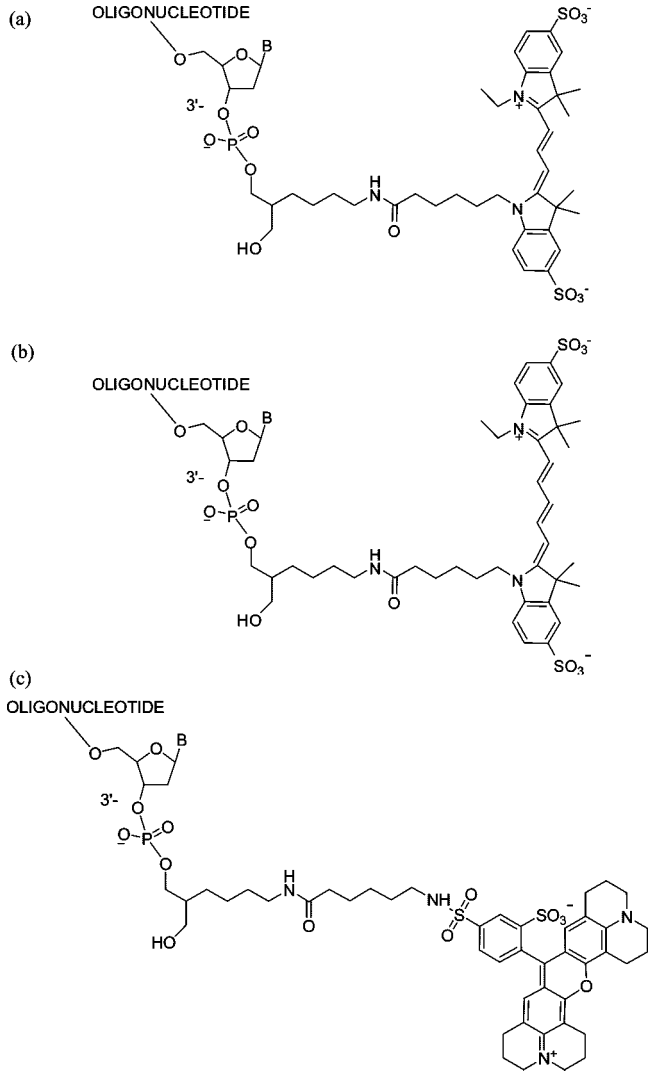

Table 1. Oligonucleotide Sequences Used in Preliminary SERS Experiments

probe	XHXHXHGCAGCAAATTGCACTGGAGTGCGAG-3′-(**FAM**), where X is a disulfide monomer and H is a hexaethyleneglycol (Heg) spacer
target	3′-GTGACCTCACGCTC-5′-**Cy3**

at room temperature, and then deprotected for 1 h at 55 °C. The 3′-FAM oligonucleotide was synthesized starting from a FAM C7 column, and 3′-Cy5 and Texas Red-labeled oligonucleotides were synthesized by postsynthetic labeling of 3′-aminoalkyl oligonucleotides, which were assembled using C7-aminolink solid support. These oligonucleotides were then labeled with the appropriate dye NHS ester (Scheme 1) as described below. The labeled probe and target sequences used in the preliminary SERS experiments are given in Table 1.

To incorporate the Cy3, Cy5, or Texas Red chromophores at the 3′-end of C7-aminoalkyl oligonucleotide, 50−150 nmol of the oligonucleotide in 70 μL of 0.5 M $Na_2CO_3/NaHCO_3$ buffer (pH 8.75) was incubated for 4 h at room temperature with 1 mg of the succinimidyl ester of Cy3, Cy5, or Texas Red (Invitrogen) in 40 μL of DMSO. The crude oligonucleotides were purified by reversed-phase HPLC and desalted by NAP-10 gel-filtration according to the manufacturer's instructions (GE Healthcare). Reversed-phase HPLC purification was carried out on a Gilson system using an ABI Aquapore column (C8), 8 mm × 250 mm, pore size 300 Å. The following protocols were used: run time 30 min, flow rate 4 mL per min, binary system, gradient, time in min (% buffer B), 0 (0); 3 (0); 5 (10); 21 (40); 21 (60); 25 (100); 27 (0); 30 (0). Elution buffer A: 0.1 M ammonium acetate, pH 7.0. Buffer B: 0.1 M ammonium acetate with 50% acetonitrile pH 7.0. (The % buffer B at 21 min was 40% for all oligonucleotides except those containing the hydrophobic Cy3, Cy5, and Texas Red dyes, which required 60% buffer B.) Elution of oligonucleotides was monitored by ultraviolet absorption at 295 nm. Texas Red oligonucleotides gave two product peaks corresponding to the 5- and 6-regioisomers of Texas Red. The first peak (5-isomer) was collected and used in the subsequent SERS experiments, and the second peak was discarded. After HPLC purification, oligonucleotides were desalted using NAP-10 Sephadex columns (GE Healthcare), aliquoted into eppendorf tubes, and stored at −20 °C. All oligonucleotides were characterized by MALDI-TOF mass spectrometry.

PCR Amplification. For the SERS-melting experiments with PCR amplicons, a synthetic DNA template (50 ng) containing the wild-type sequence or the ΔF 508 mutation was amplified in a sample volume of 20 μL, containing 0.2 μM 5′ Cy5-labeled forward primer, 0.05 μM reverse primer, 1 mM dNTPs (Promega, UK), 2.5 mM $MgCl_2$, and 1 unit hot start DNA polymerase (Eppendorf HotMaster) in 1 × PCR buffer. The PCR reactions were performed using a thermocycler (Eppendorf Mastercycler Gradient) with a denaturation step of 95 °C for 2 min, followed by 15 cycles of 94 °C for 20 s, 54 °C for 45 s, and 70 °C for 45 s. The sequences used and amplified along with that of the probe immobilized on the surface for detecting the amplicons are shown in Table 2.

Immobilization of Probe Oligonucleotides on the Substrate. The dithiol-modified oligonucleotides were diluted to 1 μM concentration with pH 8.1 phosphate buffer containing 0.1 M NaCl. It was extremely important that the substrates were clean. This was ensured by thoroughly cleaning them by sonicating in DMF for at least 3 h. Thereafter, they were immediately transferred to deionized water and sonicated for another 15 min. The substrates were preserved in water until used. For immobilizing the probe oligonucleotides, the substrates were dipped in the 1 μM solutions and kept in a refrigerator maintained at 6 °C for 48 h. After this, the substrates were taken out and washed with pH 8.1 phosphate (0.1 M NaCl) buffer several times and dipped in 10 μM mercaptohexanol solution prepared in pH 8.1 phosphate (1 M NaCl) buffer for 20 min. This ensured that any nonspecific binding of the target oligonucleotides with the substrate was prevented. The substrates were taken out and rinsed with pH 8.1 phosphate (0.1 M NaCl) buffer several times and employed for detection or mutation analysis.

Surface Coverage Determination of Probe on Gold Surface. The coulometric procedure of Steel et al.[75] using $[Ru(NH_3)_6]^{3+}$ was used to determine the coverage of immobilized probes on the gold surfaces. In this method, the $[Ru(NH_3)_6]^{3+}$ cation binds electrostatically to the phosphate groups on the DNA. Under saturating conditions, assuming that the charge on the phosphate groups is entirely compensated by $[Ru(NH_3)_6]^{3+}$, the amount of DNA bound at the surface can be deduced. This is done by measuring the charge required to reduce the DNA bound $[Ru(NH_3)_6]^{3+}$ using a short reductive potential pulse. Thus, a 500 ms pulse from an initial potential of 0.1 to −0.4 V vs SCE was employed to completely reduce the $[Ru(NH_3)_6]^{3+}$, and the charge transient was recorded. Prior to the application of the potential pulse, the solutions were deoxygenated by purging with argon for 20 min and thereafter blanketed with argon during the experiment. The electrode was allowed to equilibrate for 2 min with the solution at each concentration of $[Ru(NH_3)_6]^{3+}$ before recording the transient.

SERS-*T*melting Procedure. The thermally induced melting experiments were carried out in custom designed micro-Raman cell (Ventacon Ltd., www.ventacon.com). It utilizes a horizontal

(75) Steel, A. B.; Herne, T. M.; Tarlov, M. J. *Anal. Chem.* **1998**, *70*, 4670.

Table 2. Oligonucleotide Sequences for PCR, the Products, and the Probe Used in the Detection of Amplicons

oligonucleotide	sequence
forward primer	**Cy5**-GTATCTATATTCATCATAGGAAACACC
reverse primer	CATTGGAAGAATTTCATTCTGTTCTCAG
wild-type template	GCACATTGGAAGAATTTCATTCTGTTCTCAGTTTTCCTGGATTATGCCTGGCACCATTAAA**GAAAATATCATC-TTTGGTGTTTCCT**ATGATGAATATAGATACAGA
mutant template(ΔF 508)	GCACATTGGAAGAATTTCATTCTGTTCTCAGTTTTCCTGGATTATGCCTGGCACCATTAAA**GAAAATAT-CATC---GGTGTTTCCT**ATGATGAATATAGATACAGA
wild-type amplicon	**Cy5-**5′-GTATCTATATTCATCAT**AGGAAACACCAAAGATGATATTTTC**TTTAATGGTGCCAGGCATAATCCAG-GAAAACTGAGAACAGAATGAAATTCTTCCAATG-3′
mutant amplicon	**Cy5-**5′-GTATCTATATTCATCAT**AGGAAACACC---GATGATATTTTC**TTTAATGGTGCCAGGCATAATCCAGG-AAAACTGAGAACAGAATGAAATTCTTCCAATG-3′
probe for amplicons	$(dithiol)_3$-3′-TCCTTTGTGGTTTCTACTATAAAAG-5′

geometry for viewing under the Raman microscope, maintaining a thin 150 μm liquid film on the substrate. It is possible to flow solutions over the substrate during an experiment without disturbing the position of the substrate. A heating element is provided in the body of the cell and can be controlled with a microcontroller circuit. Two thermocouple probes are incorporated, with digital display, for controlling and monitoring the heating temperature and the temperature of the substrate, respectively. In the thermal melting, the temperature was ramped up from room temperature at 1 °C per minute to 60 °C or as appropriate in pH 8.1, 0.01 M phosphate buffer containing 0.1 M NaCl. The temperature of the substrate was recorded at the time the acquisition of each Raman spectrum was started.

SERS-*E*melting Procedure. The procedure for electrochemical melting was essentially similar to that used in *T*melting except that the temperature was held constant. The electrochemically induced melting experiments were carried out in the same custom designed micro-Raman cell. For the *E*melting experiments, the reference (Ag/AgCl) and counter (platinum wire) electrodes are placed on the side.

For a typical *E*melting experiment, the substrates were dipped in pH 7, 10 mM TRIS buffer, and the buffer was flushed over the substrates several times in the cell at open circuit potential. The experiments were carried out at room temperature. All electrochemical studies were carried out employing an EcoChemie μAutolabIII potentiostat/galvanostat. A potential sequence was applied, typically starting at -0.2 V and then -0.4 V, followed by 100 mV decrements until -1.3 V or less. The potential was held at each step for 300 s. Raman spectra were also recorded every 300 s with the first spectrum recorded 250 s after the beginning of the potential pulse.

The choice of buffers is of no particular significance except that in low ionic strength buffers we expected the electrostatic effects to be more pronounced. Hence, in this work, we show the *E*melting results in 10 mM TRIS buffer. However, it is possible to obtain *E*melting profiles in a phosphate buffer containing 100 mM NaCl and also carry out *T*melting in Tris buffer.

Raman Instrumentation. Raman spectra were acquired using a ULWD 50× objective (NA: 0.5) on a Renishaw 2000 Raman microscope instrument equipped with a 632.8 nm He−Ne laser. The diameter of the laser spot in the work presented here was 1 μm. The Raman microscope system has a motorized stage with a precision XYZ stage controller. Typically, Raman spectra were acquired from a 4 μm × 4 μm or larger area on the substrate with the laser being moved 1−2 μm each time using the stage controller. This was done to avoid any bleaching effects of the dye and was aided by the fact that signals on our substrates are reproducible.

Typically, for the targets with Cy3 label, the spectra were acquired for 20−30 s; with Texas Red, the spectra were acquired for 10 s, and for Cy5-labeled oligonucleotides it was 2−10 s, under either static mode centered at 1400 or 1450 cm^{-1} or extended mode between 3200 and 400 cm^{-1} with the laser power measured at the sample being 3 mW. When presenting the results, the spectra have been normalized by the laser power and the collection times.

Data Analysis. Unless otherwise stated, the SERS spectra presented in this Article have been background corrected using a polynomial multipoint fitting function (WiRe software, Renishaw). The Raman intensities of the peaks mentioned in this work are their heights over and above the baseline. A Boltzmann function has been used to fit sigmoidal curves to the melting profiles using Origin 7.0 software, and the first derivative of the fits was used to determine the melting points (midpoint of melting curves).

SEM Images. A Philips XL30 environmental scanning electron microscope (ESEM) and a Jeol JSM 6500F thermal field emission scanning electron microscope (FESEM) were used for taking the images of the structured substrates.

Results

Preparation of DNA SSV Surfaces. The gold sphere segment void (SSV) surfaces were made by electrodeposition of 480 nm of gold through a close-packed template of 600 nm diameter polystyrene spheres assembled on an evaporated gold surface. Efficient surface enhancement on the SSV surface requires coupling of both the incoming laser excitation and the outgoing, Stokes shifted, light to surface plasmons on the structured metal surface.[58,76] It is therefore important to choose an appropriate film thickness and sphere diameter. In this case, the values were selected to be resonant with 633 nm excitation (see Supporting Information) on the basis of earlier studies in aqueous solution.[56] Removal of the template spheres leaves the surface structured as shown in Figure 1a. SEM and voltammetric studies show that the surface of the templated structure is smooth with a surface roughness that is lower than that of the original evaporated gold film.

Single-strand DNA probe sequences, Figure 1b, were attached to the surface through three dithiol linkages and hexaethyleneglycol (HEG) spacers (Scheme 2) attached at the 5′ end of the oligonucleotide sequence by soaking the clean SSV surfaces in a 1 μM solution of the probe in pH 8.1 phosphate buffer containing 0.1 M NaCl at 6 °C for 48 h. The 6 thiol groups on the linker ensure strong binding of the DNA to the surface. For efficient hybridization with target strands from the solution, it is important to ensure that the probe sequences are not too closely packed on the surface,[77,78] and the immobilization conditions used here were chosen for that reason. The large footprint of the disulfide monomers and HEG spacers between them ensures that the surface bound probes are well spaced on the surface with enough room between them to prevent any cross-hybridization and to ensure efficient hybridization with

(76) Baumberg, J. J.; Kelf, T. A.; Sugawara, Y.; Cintra, S.; Abdelsalam, M. E.; Bartlett, P. N.; Russell, A. E. *Nano Lett.* **2005**, *5*, 2262.
(77) Herne, T. M.; Tarlov, M. J. *J. Am. Chem. Soc.* **1997**, *119*, 8916.
(78) Peterson, A. W.; Heaton, R. J.; Georgiadis, R. M. *Nucleic Acids Res.* **2001**, *21*, 5163.

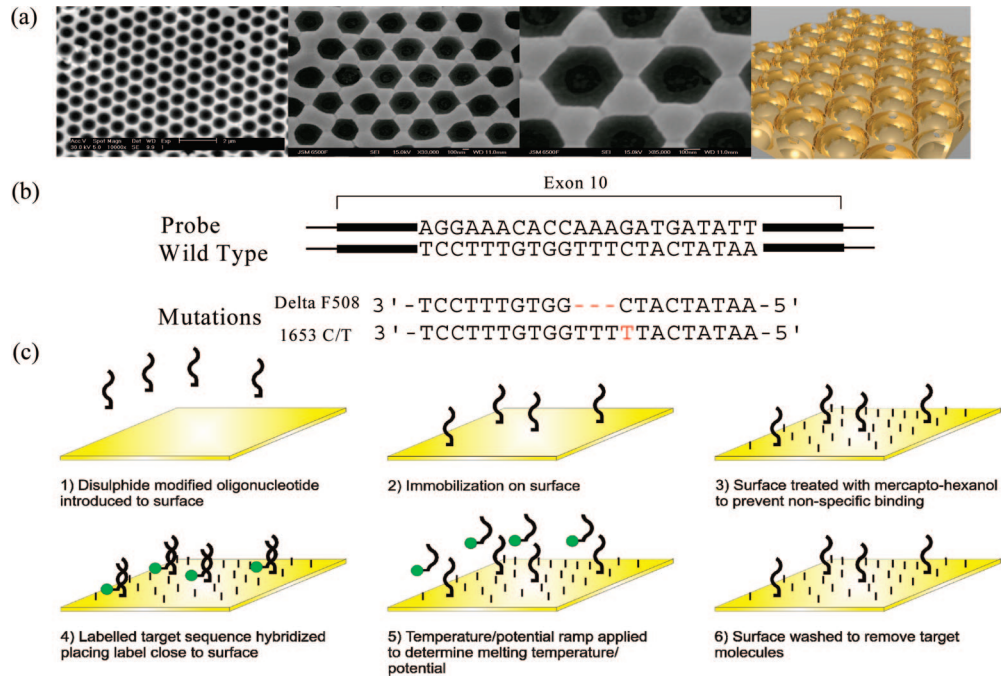

Figure 1. Substrate, scheme for detection, and sequences used. (a) Three SEM images at different magnifications of the SSV gold substrates (templated with 600 nm spheres and electroplated to 480 nm) and (right) a 3-D model of the structure. The scale bar is 2 μm for the first SEM image and 100 nm for the other two. (b) The probe and the target CFTR sequences for the synthetic oligonucleotides. The labels were attached to the 3′ end (proximal to the surface) of the target in all cases, unless mentioned otherwise. (c) The process of detection and characterization of DNA sequences beginning with (1) and (2) preparation of the sensing surface followed by (3) passivation with mercapto-hexanol to prevent nonspecific binding, (4) detection using SER(R)S-labeled targets, (5) dehybridization with either temperature or potential, and ending with (6) regeneration of the surface for reuse starting again at step 4. The dehybridization process is the key step and yields the information that characterizes mutations.

Scheme 2. Structure of the Disulfide Linkages Attached to the 5′ End of the Probe Oligonucleotides[a]

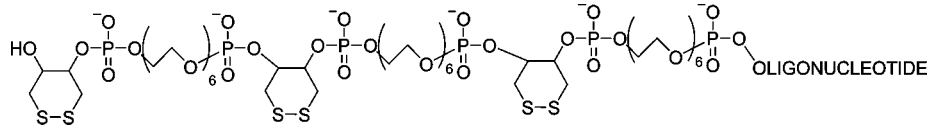

[a] The dithiol linkages ensure strong bonding with gold on immobilization.

target species from solution. Following attachment of the probe sequences, the substrates were washed and soaked in a 10 μM solution of mercapto-hexanol in pH 8.1 phosphate buffer, 1 M NaCl for 20 min, Figure 1c. The mercapto-hexanol adsorbs to the gold surface around the attached DNA and reduces nonspecific binding of target DNA from the solution at the gold surface.[77] The mercaptohexanol also has the effect of reorienting the ssDNA attached to the surface into a more upright conformation.[79,80]

Measurement of Surface Coverage. The coulometric method of Steel et al.[75] was used to determine the coverage of the immobilized DNA on the gold surfaces. Figure 2shows a typical charge transient recorded in the experiment (Figure 2a) together with the adsorption isotherm (Figure 2b). The adsorption isotherm was constructed by fitting coulometric curves of the type shown in Figure 2a recorded for different concentrations of $[Ru(NH_3)_6]^{3+}$ to the following expression for the total charge, Q,

$$Q = \frac{2nFAD_O^{1/2}c_O t^{1/2}}{\pi^{1/2}} + Q_{dl} + nFA\Gamma_O \qquad (1)$$

where t is the time, n is the number of electrons transferred, F is the Faraday constant, A is the area of the electrode, D_O is diffusion coefficient and c_O the bulk concentration of $[Ru(NH_3)_6]^{3+}$, Q_{dl} is the double layer charge, and Γ_O is the surface coverage of bound $[Ru(NH_3)_6]^{3+}$. The first term in eq 1 describes the mass transport limited reaction of $[Ru(NH_3)_6]^{3+}$ from the solution, the second term the double layer charging contribution, and the final term the contribution from the electrostatically bound $[Ru(NH_3)_6]^{3+}$. The coverage was found to be 1.6×10^{12} molecules per cm^2 so that on an average the 25 base long ssDNA molecules are 8.5 nm apart, leaving sufficient room to hybridize while preventing any cross-hybridization with target DNA from solution.

Preliminary SERS Experiments. Initial experiments were carried out using a 3′ fluorescein (FAM)-labeled 25 base long probe to test the stability and reusability of the DNA-coated SSV substrates. Figure 3 shows a set of SERS spectra recorded from the same substrate at different stages in the experiment. Spectrum a was recorded for the ssDNA immobilized on the SSV substrate at open circuit in buffer solution. The bands at 1179, 1322, and 1637 cm^{-1} correspond to the 3′ fluorescein (FAM) label[47,48] attached to the probe and are assigned to the C−OH bending, C−O phenoxide stretching, and the ring stretching vibrations, respectively.[81] There was no observable change in the spectrum when a noncomplementary 25-mer DNA labeled at the 5′ end with Cy3 was introduced into the solution,

(79) Lee, C.-Y.; Gong, P.; Harbers, G. M.; Grainger, D. W.; Castner, D. G.; Gamble, L. J. *Anal. Chem.* **2006**, *78*, 3316.
(80) Erts, D.; Polyakov, B.; Olin, H.; Tuite, E. *J. Phys. Chem. B* **2003**, *107*, 3591.

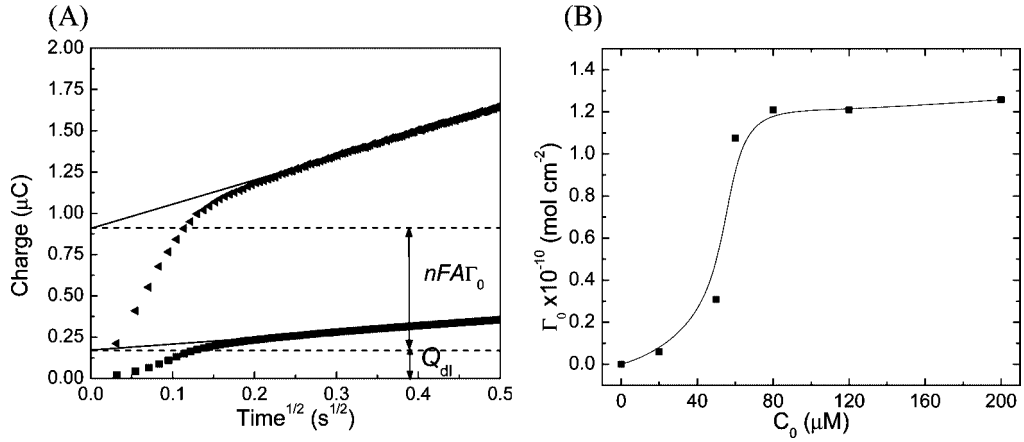

Figure 2. Coulometric determination of surface coverage of immobilized DNA. (A) Coulometric curves recorded by stepping the potential from 0.1 to −0.4 V vs SCE at a ssDNA-coated electrode (6.18 mm^2) in blank electrolyte solution (pH 7, 10 mM Tris buffer) (■) and in the same electrolyte solution containing 80 μM $[Ru(NH_3)_6]^{3+}$ (▲). (B) The adsorption isotherm for $[Ru(NH_3)_6]^{3+}$ calculated from the coulometric measurements.

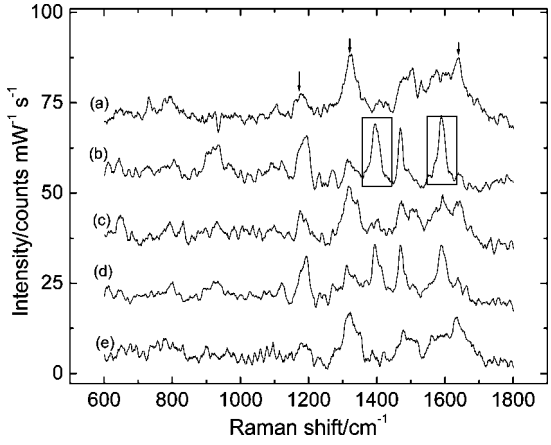

Figure 3. DNA assay and reusability. Demonstrated employing a fluorescein (FAM) 3′-labeled 25 base long probe and 14 bases long Cy3 5′-labeled target. In this study, both of the labels are at the distal end from the surface. (a) Even after incubation with a noncomplementary Cy3-labeled strand, only peaks due to FAM-labeled probe (marked with arrows) are observed in the spectrum, which is identical to that of the probe DNA alone. (b) Hybridization with a complementary Cy3-labeled target (peaks enclosed in boxes), and (d) rehybridization occurs with almost no loss in signal from Cy3-labeled target. (c and e) Dehybridization is achieved by flowing hot water (∼55 °C) for 5 min over the substrate, resulting in regeneration of the sensor substrate as inferred by the reappearance of the FAM peaks and loss of Cy3 peaks. Spectra are baseline corrected and smoothed. The spectra were recorded with an extended scan set to 30 s collection time (1 and 3 accumulations for Cy3 and FAM, respectively), 3 mW laser power in pH 8.1 phosphate buffer containing 100 mM NaCl.

confirming that the mercapto-hexanol suppresses nonspecific binding. In contrast, when the 14-mer cDNA strand labeled with Cy3 at the 5′ end is introduced into the solution the spectrum changes, Figure 3b, and new bands corresponding to the Cy3 label[35,48] appear at 1272 and 1393 cm^{-1} assigned to C−N stretch and CH deformation modes, and at 1590 cm^{-1} assigned to *C*═N stretching vibration (based on work on indocarbocyanine dyes by Sato et al.[82]). At the same time, the fluorescein bands become less prominent. We attribute the changes to the hybridization of the Cy3-labeled target to the DNA probe attached to the surface and the subsequent change in conformation of the DNA, which probably moves the 3′ fluorescein label further from the surface, thus reducing its SERS intensity.[83] In this case, the fluorescein label on the probe and the Cy3 label on the target are on the same end distal to the surface; yet the intensities of the fluorescein peaks are much weaker as compared to Cy3. This difference could be due to the lower Raman cross section of fluorescein as compared to Cy3 with the 633 nm laser used in this experiment. This suggests that in principle any molecule with a high Raman cross section could be employed as a label in these experiments. On the basis of the measured coverage of DNA on the surface and given the area illuminated by the 1 μm diameter laser spot in the spectrometer, we calculate that the spectra are recorded from approximately 12 500 molecules, giving a sensitivity of detection by SER(R)S of better than 0.02 amol. Note this is not the same as the limit of detection of the method for DNA in solution because this will also depend on the hybridization step. To test the stability of the system, the dsDNA was dehydridized by washing the surface with water at ∼55 °C for 5 min, Figure 3c, then rehybridized to the complementary target, spectrum d, and finally dehybridized with hot water again, spectrum e. Comparing the spectra in Figure 3, we can see that on dehybridization the original spectrum for the fluorescein (FAM)-labeled probe is recovered, compare spectra (a), (c), and (e), with very similar intensities. Comparing spectra (b) and (d) in Figure 3, we also find excellent reproducibility in the hybridization of the target with very similar spectral intensities of the Cy3 peaks in the two cases.

These preliminary experiments show that SERS detection on the SSV substrates gives excellent sensitivity, that we can clearly distinguish the signals of the two different dye labels, fluorescein (FAM) and Cy3, that attachment of the probe to the gold surface through the 6 thiols (3 disulfides) is robust, that the mercapto-hexanol prevents nonspecific binding of labeled DNA to the surface, and that the surfaces are reuseable.

Discrimination of Mutations by Thermal Melting. The allele-specific 22-mer probes for detecting the wild type and mutated sequences in the CFTR gene were synthesized with three dithiol linkages (Scheme 2) at the 5′-end for attachment to the gold surface. Similarly, the oligonucleotide targets were synthesized by standard solid-phase techniques and labeled at the 3′-end

(81) Wang, L.; Roitberg, A.; Meuse, C.; Gaigalas, A. K. *Spectrochim. Acta, Part A* **2001**, *57*, 1781.
(82) Sato, H.; Kawasaki, M.; Kasatani, K.; Katsumata, M.-A. *J. Raman Spectrosc.* **1988**, *19*, 129.
(83) Ye, Q.; Fang, J.; Sun, L. *J. Phys. Chem. B* **1997**, *101*, 8221.

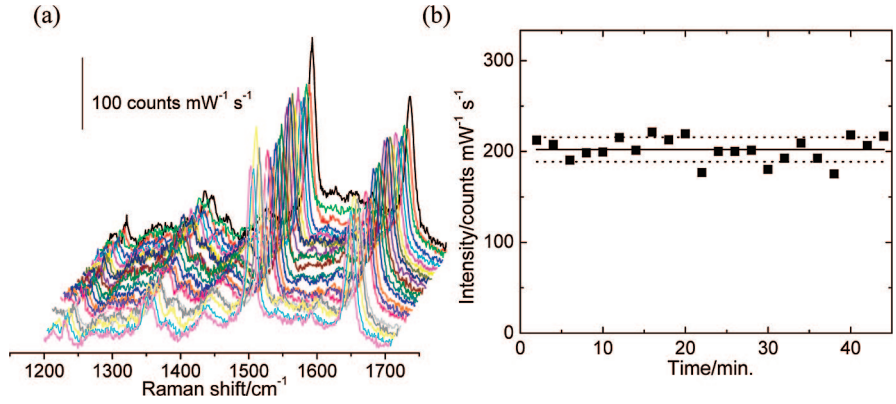

Figure 4. Reproducibility on the substrate with time. (a) Spectra of a Texas Red-labeled target with a single mismatch (1653 C/T point mutation) after hybridization recorded on a SSV substrate recorded in blank pH 8.1, 0.01 M phosphate buffer containing 100 mM NaCl. The laser spot was moved 2 μm every ~2 min while recording the spectra in static mode with a single 10 s exposure at 3 mW laser power. All spectra have been baseline corrected. (b) The peak intensity for the 1500 cm^{-1} band attributed to ring stretching mode of Texas Red plotted as a function of time for the different spectra in (a); the solid and the dotted lines show the average and std dev (7%) range, respectively. The spectra were acquired at room temperature and open circuit potential.

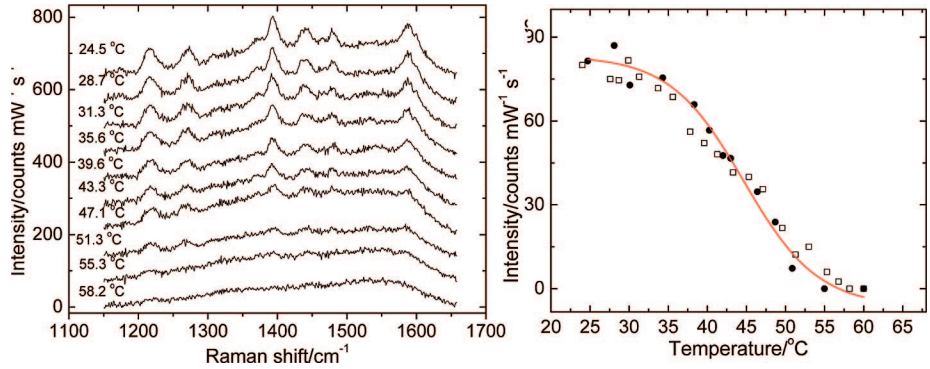

Figure 5. SERS-*T*melting experiment. (a) A sequential set of spectra recorded at different temperatures in a thermally induced dehybridization experiment using the Cy3-labeled wild-type CFTR target sequence. The temperature of the sample was ramped at 1 °C min^{-1} in blank pH 8.1, 0.01 M phosphate buffer containing 100 mM NaCl. All spectra are baseline corrected by a straight line offset between the extremities. (b) Plot of the intensity of the 1437 cm^{-1} SERS band, corresponding to the −CH asymmetric deformation mode of the Cy3 label, as a function of temperature. Data for two consecutive replicate measurements on the same substrate are shown. Spectra were acquired under a single static scan for 20 s at 3 mW laser power.

with common fluorophores, which served as SERS labels. In this case, 3′ labeling brings the label closer to surface, which is expected to increase the SER(R)S signals. The synthetic probe and target sequences are shown in Figure 1b.

The targets were detected in a hybridization assay; the entire scheme for detection and mutation discrimination is shown in Figure 1c. SER(R)S detection was carried out in a custom-made cell with electrochemical and temperature control. Hybridization was carried out in 10 μM solutions of the labeled targets in pH 8.1 phosphate buffer containing 0.1 M NaCl for 30 min. Thereafter, the substrates were rinsed by flushing the cell with the buffer at least 3 to 4 times. In experiments to discriminate mutations, the same substrate was used each time with the different targets, and spectra were collected from the same area on the substrate, although for each spectrum the laser spot was moved by 1−2 μm. This not only reduced any bleaching and photodegradation effects but also serves to demonstrate that the SERS sensitivity, surface modification, and melting effects are reproducible across the SSV surface. In fact, the substrates are reusable, and no change in melting characteristics was observed on repeated measurements. Figure 4a shows a set of 22 spectra recorded for the Texas Red-labeled 1653 C/T point mutation target hybridized to the probe on the SSV surface in the blank buffer solution at room temperature (~23 °C). The bands at 1500 and 1643 cm^{-1} correspond to the Texas Red dye[35] and are assigned to the ring stretching and −NH deformation modes in the molecule. The spectra were recorded by moving the laser spot sequentially across the surface, and again each spectrum is recorded from around 12 500 molecules in a single 10 s exposure without any spectral averaging. Texas Red has an absorption maximum at 596 nm; therefore, it is in preresonance (see Supporting Information) with the 633 nm laser used here. Figure 4b shows a plot of the intensity of the 1500 cm^{-1} band as a function of time for the set of spectra recorded at different places on the surface. The results show excellent reproducibility and stability, <7% variation.

When the temperature is increased the dsDNA begins to melt, or dehybridize, and the temperature at which this occurs will be lower if there are mismatches between the target and the probe. In the next set of experiments, the temperature was ramped at 1 °C min^{-1}, and a series of spectra were recorded at different temperatures; Figure 5a shows a representative set of data recorded for the Cy3-labeled wild-type CFTR sequence recorded in pH 8.1, 0.01 M phosphate buffer containing 100 mM NaCl. As before, the bands at 1216, 1393, 1437, 1479, and 1589 cm^{-1} are characteristic for the Cy3 label, although the intensity pattern of the peaks in this case with the label on the 3′ end is different as compared to that observed in the case of 5′-labeled target in Figure 3. Also, the signal-to-noise for the 3′-Cy3 peaks in this case is higher than that in the earlier

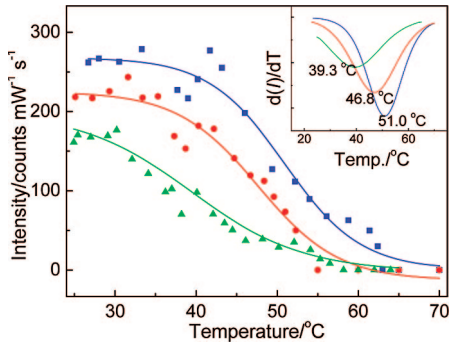

Figure 6. Thermally induced dehybridization monitored with SERS (SERS-*T*melting). The SERS intensity of the 1500 cm^{-1} band of the Texas Red label for the three targets, (■) wild type (no mutation), (●) 1653C/T mutation (single point mutation), and (▲) Δ*F* 508 mutation (triple deletion), is plotted against the temperature. The first derivatives of the sigmoidal fits of the intensity curves are shown in the inset. The temperature of the sample was ramped at 1 °C min^{-1} in blank pH 8.1, 0.01 M phosphate buffer containing 100 mM NaCl. Spectra were acquired in static mode with a single 10 s exposure at 3 mW laser power on the same substrate beginning with the triple deletion, followed by the single point mutation and then the perfect match.

experiments. As the temperature increases, we can see that the intensity of the Cy3 bands decreases sequentially, eventually disappearing at high temperature when all of the dsDNA has melted and the labeled target molecules diffuse away from the surface. Note that the SERS signal decreases because the enhancement is strongly surface specific; labeled DNA molecules that are not close to the surface (less than about 100 nm) do not contribute to the signal. We can analyze the thermal melting of the dsDNA on the surface by plotting the intensity of the SERS signal as a function of temperature. Figure 5b shows results for two consecutive measurements made on the same surface, showing excellent agreement in both overall signal intensity and in the temperature variation. In both cases, there is a sigmoidal drop in signal with a mid point temperature of about 45 °C. This type of SERS-*T*melting measurement is reproducible and can be used to discriminate mutations with high sensitivity.

Figure 6 shows SERS-*T*melting for the three different targets, wild type and two mutations each labeled with Texas Red. As expected, the wild type, which is a perfect match for the probe, melts at the highest temperature, while the Δ*F* 508 triple deletion, which is the worst match, melts at the lowest temperature. Analysis of the melting curves gives melting temperatures (T_m), which show a difference of 4.2 °C for the single point mutation and 11.7 °C for the triple deletion as compared to the wild type. It is also noticeable that the triple deletion shows the lowest SERS intensity at all temperatures, possibly indicating lower surface coverage as a result of weaker binding to the probe. Again, these spectra were acquired from around 12 500 molecules on the surface, demonstrating that SERS-*T*melting on the SSV substrate is a very sensitive method to discriminate single nucleotide mutations.

Discrimination of Mutations by Electrochemical Melting. The results presented above show that SERS at the SSV substrates is a very sensitive method to discriminate mutations by recording spectra as the temperature is increased. However, close control over the temperature and reproducible heating of the system requires special equipment and cannot be applied selectively to one region of a surface and not to a nearby region. We therefore also investigated the effects of using the SSV substrate as an electrode and slow ramping of its potential.

In a typical SERS-electrochemical-melting (SERS-*E*melting) experiment, after hybridization with the target the cell was flushed several times with 10 mM TRIS buffer, pH 7, and the surface was equilibrated at open circuit potential for several minutes. Thereafter, the SSV electrode was potentiostatted and the potential decreased in steps from −0.2 to −1.5 V vs Ag/AgCl. SER spectra were recorded at each potential step after a fixed time interval of 250 s. A typical SERS-*E*melting analysis in the present, unoptimized form therefore took less than an hour. Figure 7 shows results for a SERS-*E*melting experiment using the same probes and the same three Texas Red-labeled targets as in the SERS-*T*melting experiment shown in Figure 6. As the potential is taken cathodic, Figure 7a, we see that the bands at 1500 and 1643 cm^{-1} characteristic of the Texas Red label first increase and then decrease in intensity, eventually disappearing at the most cathodic potential. It is notable that the spectra are again much clearer than in the spectra presented in Figure 3. This is because Texas Red is in preresonance with the 633 nm laser, resulting in an additional resonance enhancement over and above the surface enhancement. Plotting the extracted SERS intensities of the Texas Red aromatic ring stretching band at 1500 cm^{-1} against potential yields the SERS-*E*melting profiles, which are shown in Figure 7b. The first derivatives of the sigmoidal curve fits to the melting curves (inset) were used to define the melting potentials (E_m). As evident in Figure 7b, the profiles for the perfect match and the two mutations are clearly distinguishable with shifts in the melting potentials (ΔE_m) of 110 and 60 mV, respectively. Again, as expected, the mutation with the triple deletion is the least stable and shows the most positive melting potential. In all cases, the intensity of the peak for the SERS marker increases as the potential becomes more negative from −0.2 to −0.8 V before then decreasing and ultimately falling to zero at potentials more negative than −0.8 V. The initial increase is reversible, and we speculate that this is due to a potential-dependent change in the orientation of the dsDNA and the 3′ Texas Red label. This requires further study, but it is worth noting that we do not see the same effect when we use Cy5 as a label or in the case of thermal melting with either of the dyes; see Figure 9 and discussion below.

Reproducibility of SERS-*E*melting. Figure 8 shows results for consecutive SERS-*E*melting experiments using the same SSV substrate and the Texas Red-labeled Δ*F* 508 target. After the first SERS-*E*melting measurement, the substrate was stored in buffer solution for 3 days and then rehybridized with the same target. There is good reproducibility in both the intensity profiles of the SERS signal and the *E*melting characteristic with excellent agreement in the melting potential, E_m, for the two measurements. These results show that the loss of SERS signal at high cathodic potentials arises from melting of the dsDNA and loss of labeled target from the surface and not through reductive desorption of the DNA probe (reductive desorption can occur in our experiments, but it does not become significant until the potential is taken more negative than −1.3 V vs Ag/AgCl). These results demonstrate the excellent reusability of these surfaces for DNA detection and mutation discrimination and also show the stability and reproducibility of the SSV gold SERS substrates used in this work.

Potential Dependence of the SERS Spectra. SER(R)S spectra are quite rich in information about changes in orientation and can in principle be used to study the melting process in detail.

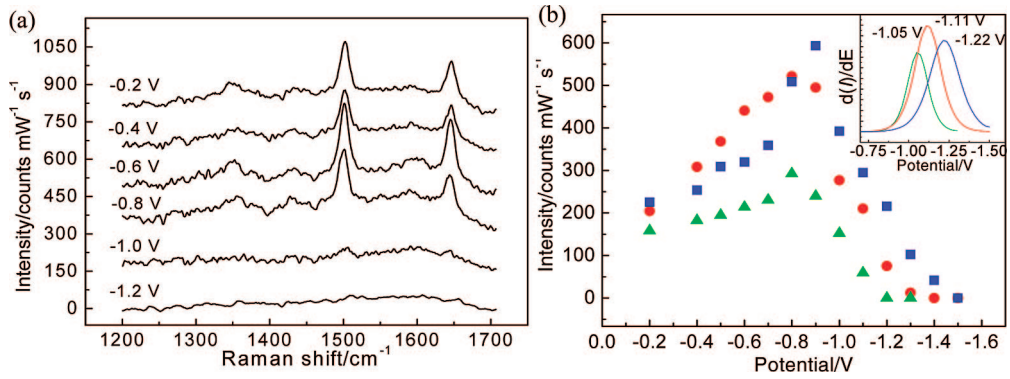

Figure 7. Electrochemical dehybridization monitored with SERS (SERS-*E*melting) for mutation discrimination. (a) Representative spectra of Texas Red-labeled Δ*F* 508 synthetic target at various potentials in an actual SERS-*E*melting experiment with the intensity of peaks changing with applied potential. (b) The SERS intensities of the 1500 cm^{-1} band of the dye label (Texas Red) for the three targets, (■) wild type (no mutation), the (●) 1653C/T mutation (single point mutation), and the (▲) Δ*F* 508 mutation (triple deletion), are plotted against the applied potential. The first derivatives of the sigmoidal fits of the intensity curves are shown in the inset with the melting potentials shown above each curve. Spectra were acquired in static mode with a single 10 s exposure at 3 mW laser power on the same substrate beginning with the triple deletion, followed by the single point mutation and then the perfect match, in pH 7, 10 mM Tris buffer.

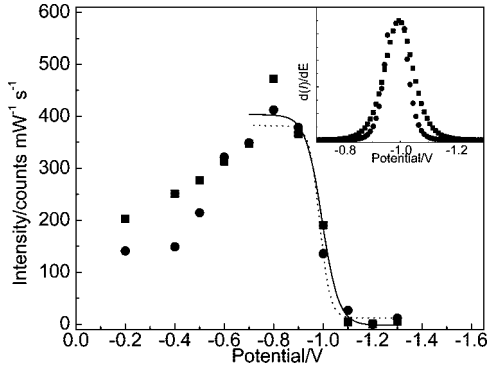

Figure 8. Reproducibility of SERS-*E*melting. The peak intensities for the 1500 cm^{-1} band for Texas Red-labeled Δ*F* 508 target oligonucleotides are plotted as the function of potential for two successive measurements carried out 3 days apart on the same DNA probe-modified SSV substrate (■ first run, ● second run). The dehybridization profiles are reproducible on the substrates with almost no variation in the melting potential values, 0.99 and 0.98 V, respectively (the first derivatives of the fitted profiles are shown in the inset). Spectra were acquired in static mode with a single 10 s exposure at 3 mW laser power in pH 7, 10 mM Tris buffer.

Figure 9a shows a set of SERRS (also called resonant SERS) spectra recorded at different potentials for the 3′ Cy5-labeled complementary target hybridized to the immobilized probe on the SSV surface. Cy5 is a cyanine dye with an absorption maximum of 647 nm (see Supporting Information). It is therefore resonant with the 633 nm laser used in these experiments, and so, as expected, the signals in the SERR spectra of this label are significantly more intense (in this case by a factor of 4−5) than those for the partially resonant Texas Red label shown in Figure 7. The bands at 583 and 935 cm^{-1} are assigned to alkene chain and aromatic CH deformation modes, and those at 1367 and 1597 cm^{-1} to methine chain deformation and *C*═N stretching modes, respectively, and are characteristic of Cy5.[35] Figure 9b shows normalized melting profiles calculated from four different bands in the Cy5 spectrum. In each case, the intensity of the band decreases as the potential moves cathodic, but it is noticeable that there are no significant shifts in band position. The melting profiles derived from each band may give some information about the conformational changes that accompany partial melting of the dsDNA. This is an area that deserves further study.

With Cy5 as the label, the electrochemical melting profile is shifted 400−450 mV less negative, depending on which band we take, as compared to the value for the corresponding Texas Red-labeled target (Figure 7). Thus, the particular choice of the label has a significant effect on the stability of the surface bound dsDNA. At neutral pH, Cy5 is a dianion whereas Texas Red is a zwitterion; we speculate that the difference in the SERS-*E*melting profiles is caused by the additional negative charge on the Cy5 label at the 3′ end of the target leading to dehybridization at lower potentials and temperatures (data not shown). The melting temperature of the perfect match with 3′ Cy5 label was found to be 45 °C, which is 6 °C lower than that measured for the corresponding 3′ Texas Red-labeled target. We also note that for the Cy5-labeled system the initial increase in SER(R)S intensity observed with Texas Red (Figure 7b) is not found but that the melting profiles for Texas Red-labeled oligonucleotides are sharper as compared to Cy5-labeled sequences. These effects highlight the possibility of optimizing the choice of SER(R)S label in future work.

Application of SERS-*E*melting to Analysis of PCR Products. The examples described above clearly demonstrate that there are readily measurable differences in the SERS-melting responses and that discrimination of mutations is possible for a model system. To demonstrate the potential practical utility of the method, we carried out mutation discrimination experiments with PCR products of the wild type and Δ*F* 508 mutated sequences from the CFTR gene. The primers in this case were labeled with Cy5, and the surface bound probe sequence was redesigned (see Table 2). For the PCR product, the target strand is much longer; we use a 103-mer as compared to the synthetic 22-mer oligonucleotides used above. When hybridized to the probe sequence on the surface, the PCR product has overhanging sequences at both ends with a 15 base long nonoverlapping part of the primer on the 3′-end.

Figure 10 shows results for the SERS-*E*melting experiment with the PCR product. The target solution was as obtained after PCR without any purification; hence, it contained residual dNTPs, primer, $MgCl_2$, and DNA polymerase besides the amplicon. In comparison with the results in Figure 9, the positions of several of the Cy5 bands are shifted (see Supporting Information); this is because a 5′-Cy5 phosphoramidite label was used in this case rather than the 3′-Cy5 added as an NHS

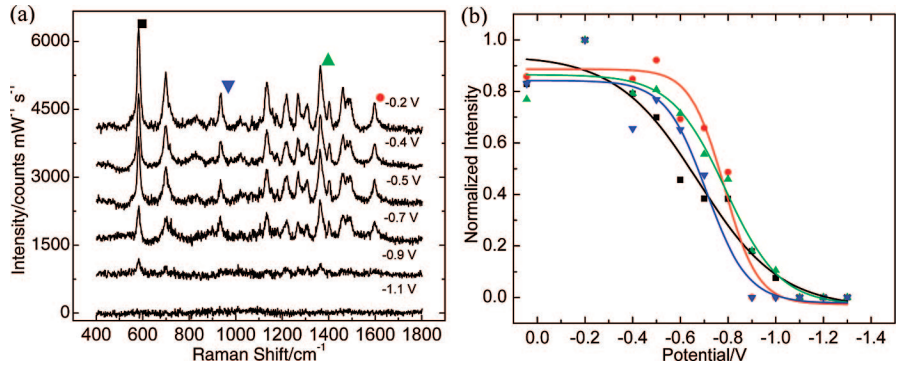

Figure 9. (a) SERRS (or resonant SERS) spectra of Cy5-labeled complementary strand recorded at the different potentials indicated beside each spectrum. The spectra are offset for clarity. (b) Normalized resonant SERS-*E*melting profiles extracted from the SERRS bands at (■) 583 cm^{-1}, (▼) 935 cm^{-1}, (▲) 1367 cm^{-1}, and (●) 1597 cm^{-1} for the Cy5-labeled synthetic target strand. Spectra were acquired in the extended mode with a single scan set to 3 s collection time at 3 mW laser power in pH 7, 10 mM Tris buffer.

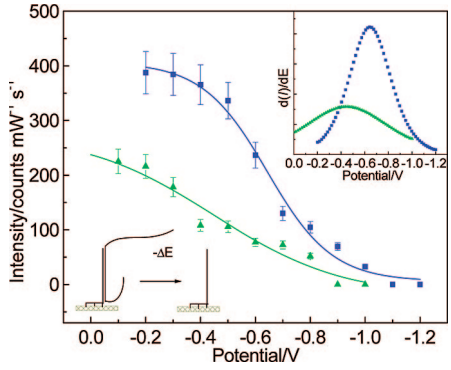

Figure 10. The resonant SERS-melting profiles of the PCR products for wild type (■) and Δ*F* 508 mutation (▲) using the 1347 cm^{-1} SERRS (resonant SERS) band for Cy5. A schematic of the dehybridization process of the PCR products is shown. The first derivatives of the melting profiles are shown in the inset. The mutation has a melting potential of −0.44 V, while that of the wild type is −0.64 V vs SCE. Spectra were acquired with a single static scan of 2 s exposure at 1.5 mW laser power in pH 7, 10 mM Tris buffer.

ester. Once again, there is still a significant difference of 200 mV between the melting potential (ΔE_m) of the mutation and the wild type. As compared to the results for the model system, Figure 9, the melting profile is shifted to less negative potentials by about 200 mV. It is possible that this is due to the increased destabilization of the duplex at the surface due to the longer overhanging strands of the PCR product. The negative control for the PCR products was also tested with the same procedure, and no signal from the Cy5 label could be observed, confirming that there is no nonspecific binding and no contamination of the sample during PCR, which was also separately confirmed by gel electrophoresis.

Discussion

Thermal melting of dsDNA to discriminate mutations is usually applied in solution with fluorescence monitoring rather than to surface bound DNA, although such approaches have been used in microarrays. Our thermal melting study demonstrates the first use of in situ SER(R)S dehybridization of dsDNA, which we show can be employed for distinguishing mutations. Peterlinz et al.[65] have described the application of thermal melting to dsDNA attached to a gold surface followed by SPR where they showed a clear difference in the melting temperature depending on the electrolyte concentration but did not discriminate between different DNA target strands. In our case, as described above, the approach shows excellent selectivity for single point mutations and excellent sensitivity. This is in large part due to the high sensitivity of the SER(R)S technique coupled to the excellent stability of our SSV substrates, which provide a stable SERS enhancement, even when the temperature is cycled and the substrates are reused, and the robust attachment of the probe DNA through the six thiol (three disulfide) linkages.

Although the SERS-*T*melting method works well, the SERS-*E*melting approach has significant advantages because potential control can be localized more easily and is therefore more suitable for miniaturization, addressability, integration with integrated circuit (IC) technology, and lower implementation costs than is precise temperature control. The use of applied potential to direct or in some way control the immobilization, hydridization, or denaturation of DNA has a long history. As early as 1957, Hill[84] pointed out, based on a statistical thermodynamic treatment, that the stability of double-stranded DNA should be affected by an electric field and predicted that fields of the order of 10^4 V cm^{-1} could bring about melting of dsDNA. Early work on the electrochemistry of calf thymus DNA at mercury electrodes[85,86] provided evidence, based on the accessibility or otherwise of cytosine and adenine nucleotides for reduction at mercury, for partial melting of dsDNA at around −1.2 V vs SCE. In this case, the dsDNA was assumed to be adsorbed parallel to the electrode surface so that it experienced the full effect of the potential drop across the double layer at the electrode surface.

There have been a limited number of studies of field effects on the immobilization,[78,87] hybridization,[64,88] or denaturation[64,71−73,89] of DNA directly attached to electrode surfaces. A significant increase in the rate of hybridization was found by Heaton et al.[64] in a study of the reaction of target DNA sequences with probe sequences attached to a gold surface through a thiol link. In the same paper, they also show that denaturation of dsDNA at the surface can be driven by the potential. In these experiments, they found that a fixed potential of −0.3 V led to the denaturation of a two base mismatched target strand from the

(84) Hill, T. L. *J. Am. Chem. Soc.* **1958**, *80*, 2142.
(85) Brabec, V.; Paleček, E. *Biophys. Chem.* **1976**, *4*, 79.
(86) Valenta, P.; Nürnberg, H. W. *Biophys. Struct. Mech.* **1974**, *1*, 17.
(87) Ge, C.; Liao, J.; Yu, W.; Gu, N. *Biosens. Bioelectron.* **2003**, *18*, 53.
(88) Su, H.-J.; Surrey, S.; McKenzie, S. E.; Fortina, P.; Graves, D. J. *Electrophoresis* **2002**, *23*, 1551.
(89) Wei, F.; Sun, B.; Liao, W.; Ouyang, J.; Zhao, X. S. *Biosens. Bioelectron.* **2003**, *18*, 1149.

probe in the hybridization buffer in a few minutes, whereas there was little loss of the fully complementary strand over several hours. A similar effect of moderate negative potentials on the rate of denaturation was observed by Spehar-Deleze et al.[73] using electrochemiluminescent detection at gold electrodes. In a recent series of papers, Wei et al.[71,72,89] demonstrated that scanning electrode potential could be used to discriminate single nucleotide polymorphisms using hairpin probes. In these experiments, the DNA hairpin probes were immobilized on doped p-Si (111) substrates, and experiments were carried out in 10 mM TRIS buffer containing 1 mM EDTA. Duplex dissociation was monitored either by impedance measurements[89] or by fluorescence.[71,72] Significantly, the authors found that in their experiments it was essential to use a hairpin probe and there was no discrimination when the experiment was repeated with a linear probe.[71]

It is of interest to consider the mechanism of discrimination in our experiments. The persistence length for double-stranded DNA is 80 nm,[90] significantly longer than the 25 base and 22 base long duplexes used in our experiments, which were only around 9.5 and 8.5 nm long, respectively. Thus, the dsDNA approximates to a rigid cylinder with an effective diameter, including the 0.5 nm thick countercation sheath due to Manning condensation,[91] of 3 nm attached to the gold surface through the six gold thiol bonds by a flexible hexaethyleneglycol (HEG) linkage 1.2 nm long. The measurements of surface coverage give an average surface area of 0.016 nm^2 for the 25 base long DNA probe so that, on average, the strands are 8.5 nm apart. The gold between the DNA probes is covered by a layer of mercapto-hexanol around 0.8 nm thick. Several studies using a range of techniques have established that for dsDNA immobilized on gold surfaces coimmobilized with mercapto-hexanol the DNA stands up and extends out into the solution[92,93] and that as the applied potential changes the orientation of the attached dsDNA can be switched from near the surface at potentials close to the potential of zero charge (pzc) to perpendicular to the surface at potentials negative of the pzc.[94,95] Thus, we can picture the dsDNA at the electrode surface at the negative potentials where the electrochemically driven denaturation occurs as shown in Figure 11. The reversible change in orientation of the dsDNA with applied potential reported in the literature[92,94,95] is consistent with the reversible changes in SERS intensity seen in Figures 7b and 8 for the Texas Red-labeled molecules. The results of our experiments are in general agreement with the thermodynamic calculations of Vainrub and Pettitt[96,97] on the electrostatic effects on DNA hybridization at electrode surfaces, which predict that potentials negative of the potential of zero charge should decrease the stability of the dsDNA at the electrode surface and enhance melting. This simple model partially explains our *E*melting data. In the simple Gouy−Chapman model, the bulk of the potential in the double layer at the electrode surface is dropped over the Debye

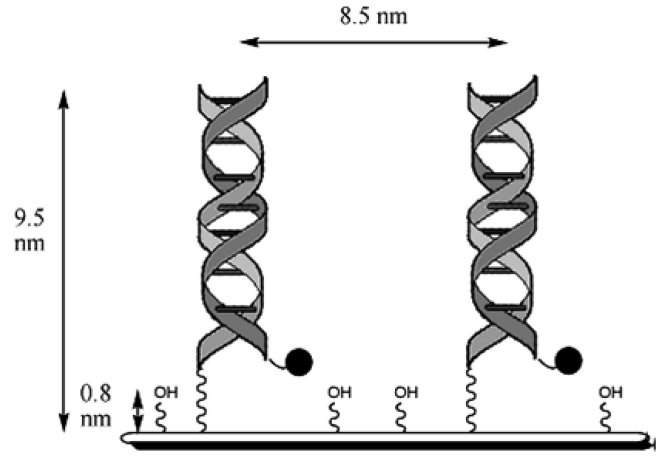

Figure 11. Schematic showing the configuration at negative electrochemical potentials on a gold surface with estimated dimensions (approximately to scale) of the distribution of the DNA sequences in the mercaptohexanol layer for a 25 base long duplex.

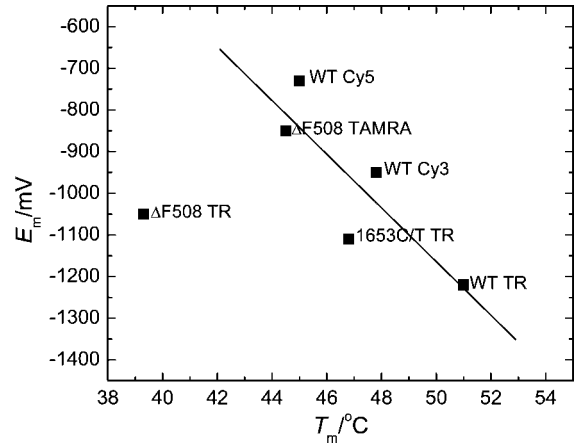

Figure 12. The melting potentials (E_m) plotted versus melting temperatures (T_m) for different targets bearing various labels determined from the SERS-melting experiments with the 22-mer oligonucleotide targets.

length,[95−97] which for our buffer solution is ∼3 nm, with the field decaying to zero over three multiples of the Debye length. Thus, in the current work most of the dsDNA might be expected to be within the double layer. However, it is possible that the *E*melting effect is not only due to the effect of the potential but also to local changes in pH caused by electrode reactions, but this seems unlikely given the large range of *E*melting potential we observe (from −0.44 V for the Cy5-labeled Δ*F* 508 PCR product to −1.22 V for Texas Red-labeled wild type). Comparing the *E*melting and *T*melting experiments, there is a reasonable correlation between the two, Figure 12, suggesting that the *E*melting effect is directly probing the thermodynamic stability of the duplex. Clearly, further work is required to understand the full details of the *E*melting process. Nevertheless, it is clear from the results presented here that it is a simple reproducible, sensitive, and accurate method to discriminate single nucleotide polymorphisms.

Conclusions

In this work, we have provided "proof of concept" of a new method for distinguishing mutations employing SERS detection

(90) Bednar, J.; Furrer, P.; Katritch, V.; Stasiak, A. Z.; Dubochet, J.; Stasiak, A. *J. Mol. Biol.* **1995**, *254*, 579.
(91) Manning, G. *Acc. Chem. Res.* **1979**, *12*, 443.
(92) Kelley, S. O.; Barton, J. K.; Jackson, N. M.; McPherson, L. D.; Potter, A. B.; Spain, E. M.; Allen, M. J.; Hill, M. G. *Langmuir* **1998**, *14*, 6781.
(93) Levicky, R.; Herne, T. M.; Tarlov, M. J.; Satija, S. K. *J. Am. Chem. Soc.* **1998**, *120*, 9787.
(94) Rant, U.; Arinaga, K.; Fujita, S.; Yokoyama, N.; Abstreiter, G.; Tornow, M. *Nano Lett.* **2004**, *4*, 2441.
(95) Rant, U.; Arinaga, K.; Fujita, S.; Yokoyama, N.; Abstreitera, G.; Tornowa, M. *Org. Biomol. Chem.* **2006**, *4*, 3448.
(96) Vainrub, A.; Pettitt, B. M. *Chem. Phys. Lett.* **2000**, 323.
(97) Vainrub, A.; Pettitt, B. M. *Biopolymers* **2003**, *68*, 265.

(termed SERS-melting) on ordered gold sphere segment void substrates, and we have demonstrated its potential utility in a PCR-based application. Many practical applications are envisaged leveraging the advantages of SER(R)S over fluorescence and other detection methods especially in being able to combine immense molecule-specific information with high sensitivity. The other advantage of our SERS substrate approach is its fundamental suitability for high throughput analysis, miniaturization, and the possibility of multidimensional control of the denaturation process by electrochemical potential, temperature, and/or solution composition. Thus, SERS-melting could prove to be an important enabling technology in the fields of diagnostics, genomics, and forensic science.

Acknowledgment. S.M. thanks ORSAS for a scholarship.

Supporting Information Available: Reflectance spectrum of the SSV structure used in this work, absorption spectra of the dye labels, and SERRS spectra of 3′- and 5′-Cy5-labeled targets corresponding to Figures 9 and 10, respectively. This material is available free of charge via the Internet at http://pubs.acs.org.

JA805517Q